Fish and Shellfish Immunology 89 (2019) 207–216

Contents lists available at ScienceDirect

Fish and Shellfish Immunology

journal homepage: www.elsevier.com/locate/fsi

Full length article

Beclin-1 is involved in the regulation of antimicrobial peptides expression in Chinese mitten crab *Eriocheir sinensis*

Wen Yang[a], Chao Liu[a,c], Qingsong Xu[a,c], Chen Qu[a], Jiejie Sun[a], Shu Huang[a], Ning Kong[a], Xiaojing Lv[a], Zhaoqun Liu[a], Lingling Wang[a,b,c], Linsheng Song[a,b,c,*]

[a] Liaoning Key Laboratory of Marine Animal Immunology, Dalian Ocean University, Dalian, 116023, China
[b] Laboratory of Marine Fisheries Science and Food Production Process, Qingdao National Laboratory for Marine Science and Technology, Qingdao, 266235, China
[c] Liaoning Key Laboratory of Marine Animal Immunology and Disease Control, Dalian Ocean University, Dalian, 116023, China

ARTICLE INFO

Keywords:
Beclin-1
Eriocheir sinensis
Lipopolysaccharide
Antimicrobial peptides
Immune response

ABSTRACT

Beclin-1, the mammalian ortholog of yeast Atg6, plays essential roles in the regulation of various processes, including autophagy, apoptosis, embryonic development and immune responses in vertebrates. However, the information about Beclin-1 in invertebrates especially in crustaceans is still very limited. In the present study, a novel Beclin-1 (designated as *Es*Beclin-1) was identified from Chinese mitten crab *Eriocheir sinensis*. The open reading frame of *Es*Beclin-1 cDNA was of 1,275 bp, encoding a typical APG6 domain. The deduced amino acid sequence of *Es*Beclin-1 shared high similarity ranging from 42.9% to 63.6% with the previously identified Beclins. In the phylogenetic tree, *Es*Beclin-1 was firstly clustered with *Drosophila melanogaster* Atg6 and then assigned into the branch of invertebrate Beclin-1. The mRNA transcripts of *Es*Beclin-1 were highly expressed in hepatopancreas, hemocytes and gill. After lipopolysaccharide (LPS) and *Aeromonas hydrophila* stimulations, the relative mRNA expression of *Es*Beclin-1 in hemocytes was significantly increased from 3 to 24 h with the peak level of 4.70-fold ($p < 0.01$) and 2.91-fold ($p < 0.01$) at 6 h, respectively. *Es*Beclin-1 protein was diffusely distributed in the cytoplasm of crab hemocytes under normal conditions, whereas it displayed predominantly punctuate distribution after LPS stimulation. After *Es*Beclin-1 was interfered with specific *Es*Beclin-1-dsRNA, the mRNA transcripts of some antimicrobial peptides, including *Es*ALF2, *Es*LYZ, *Es*Crus and *Es*Crus2 in crab hemocytes were significantly decreased at 6 h post LPS stimulation. These results implicated that *Es*Beclin-1 played a role in regulating the antimicrobial peptides expressions in the immune responses of *E. sinensis*.

1. Introduction

Autophagy is a fundamental process that mediates the degradation of cytosolic constituents such as damaged proteins and organelles [1,2]. The autophagy-related proteins in innate immune system could coordinate cell-autonomous antimicrobial responses to against diverse pathogens [3]. The genes and proteins constituting the basic machinery of the autophagic processes were initially identified in yeast system, and some of their orthologs had also been characterized in mammals [4,5]. Beclin-1 was described as the mammalian counterpart of the yeast autophagy Apg6 (later named as Atg6/vacuolar protein sorting 30, Vps 30), which was initially characterized as a Bcl-2-interacting protein in mouse [6]. In the past two decades, Beclin-1 has aroused wide attentions and has been identified to play vital roles in diversely biological processes, including development, tumor suppression, lifespan extension, and immunity [7–9].

Beclin-1, characterized with a typical APG6 domain, is mainly consisted of other three identifiable domains, including an *N*-terminal Bcl-2 homology 3 (BH3) domain, a central coiled-coil domain (CCD), and a *C*-terminal evolutionarily conserved domain (ECD) [10,11]. BH3 domain can directly combine with anti-apoptotic Bcl-2 family members (like Bcl-2 and Bcl-XL) to facilitate the coordinative regulation of autophagy and apoptosis [12,13]. ECD is capable of interacting with class III phosphatidylinositol 3-kinase (PI3K) as a PI3K complex to initiate autophagy, and recruiting other autophagic proteins to promote the maturation of autophagosomes [4,7,14]. The central CCD is also found to be involved in autophagosomes maturation [15]. Beclin-1 plays essential roles in coordinating the cytoprotective functions of autophagy and apoptosis [16], and acts as a tumor suppressor protein in human and mouse [17,18]. Meanwhile, Beclins also play diverse roles in embryonic development, endolysosomal trafficking, and metabolism [9,19,20]. For instance, the mouse embryos with depletion of Beclin-1

* Corresponding author. Liaoning Key Laboratory of Marine Animal Immunology, Dalian Ocean University, Dalian, 116023, China.
E-mail address: lshsong@dlou.edu.cn (L. Song).

https://doi.org/10.1016/j.fsi.2019.03.065
Received 31 December 2018; Received in revised form 25 March 2019; Accepted 26 March 2019
Available online 29 March 2019

performed profound developmental delay, and even death [8]. Bec-1 was crucial for morphogenesis of the dauer larva and life-span extension mediated by insulin signaling or dietary restriction in *Caenorhabditis elegans* [21]. In *Drosophila melanogaster*, Atg6 was required for endocytosis, protein secretion, and hematopoiesis [19]. Beclin-2, the mammalian specific protein, not only functioned in autophagy, but also in endolysosomal trafficking and metabolism [20].

Recently, an increasing number of studies have indicated that Beclin-1 also plays a vital role in immune responses against pathogen infections in both vertebrates and invertebrates. For instance, the CCD of human *Hs*Beclin-1 could interact with the central NTase domain of the cytosolic DNA sensor cyclic GMP-AMP synthetase (cGAS), and result in well-balanced antimicrobial immune responses [22]. The *Cynoglossus semilaevis* Beclin-1 (*Cs*Beclin-1) participated in regulating the bacterial dissemination in head kidney and spleen [23]. *Ce*Bec-1 from *C. elegans* could successfully protect the intestinal epithelium cells from overwhelming bacterial infection and cellular destruction [24]. The overexpression of *Mm*Beclin-1 was helpful to protect mice against lethal sindbis virus encephalitis [6]. In *Paralichthys olivaceus*, *Po*Beclin-1 was involved in the immune response against viral infection [25]. A number of evidences have further declaimed the involvement of Beclin-1 in regulating the activity of NF-κB. The activation level of NF-κB in autophagy-deficient (Beclin-$1^{-/-}$ and Atg$5^{-/-}$) immortalized kidney cells of baby mouse was lower than that in autophagy-competent (Beclin-$1^{+/+}$ and Atg$5^{+/+}$) cells in response to TNF-α [26]. In human T cell leukemia virus type 1 (HTLV-1)-transformed T Lymphocytes, Beclin-1 was able to interact with the catalytic subunits of IκB kinase (IKK) via its *C*-terminus, thus functioned in maintaining Tax-induced activation of NF-κB and Stat3 [27]. Furthermore, Beclin-1 was also directly related to the canonical NF-κB activation pathway through its CCD [28]. However, the potential relations between autophagy-related genes and NF-κB pathway are not well understood in invertebrates.

Eriocheir sinensis is one of the most important aquaculture species in China [29]. With the intensification of high-intensity aquaculture and the degradation of environment, the increasing diseases caused by bacteria infections have resulted in enormously economic loss in crab aquaculture [30]. The cumulative evidences suggest that Beclin-1 can regulate NF-κB activation via the interaction with IKK in mammals. The knowledge of *E. sinensis* Beclin-1 as well as its involvement in regulating antimicrobial peptides (AMPs) production would help better understand the immune defense mechanism of crustaceans against bacterial infections. The main objectives of the present study are to (1) analyze the sequence characteristics of Beclin-1 from *E. sinensis* (designated as *Es*Beclin-1), (2) explore its tissue distribution and subcellular localization, as well as its temporal expression profiles after immune stimulations, (3) detect the expression levels of anti-lipopolysaccharide factor (*Es*ALF2), lysozyme (*Es*LYZ) and crustin (*Es*Crus and *Es*Crus2) in hemocytes after LPS stimulation in *Es*Beclin-1-interfered crabs, hopefully to validate the possible roles of Beclin-1 in regulating the innate immune response.

2. Materials and methods

2.1. Crabs, immune stimulations, and sample collections

Chinese mitten crabs *E. sinensis* with an average weight of 20 g were collected from a commercial farm in Lianyungang, China. The crabs were acclimatized in aerated water at 20 ± 2 °C for one week before processing. Gram-negative bacteria *Aeromonas hydrophila* were cultured in LB broth at 28 °C with shaking at 200 rpm.

One hundred and eight crabs were randomly divided into three groups, PBS (control) group, lipopolysaccharide (LPS) group, and *A. hydrophila* group. Crabs in the control group received an injection of 100 μL phosphate buffer (PBS, 140 mM NaCl, 2.7 mM KCl, 10 mM Na_2HPO_4, 2 mM KH_2PO_4, pH 7.4). In the experimental groups, each crab received an injection of 100 μL LPS from *Escherichia coli* 0111: B4 (Sigma Aldrich, USA, 200 μg mL^{-1} in sterile PBS) for LPS group and 100 μL A. *hydrophila* (1×10^7 CFU mL^{-1} in sterile PBS) for *A. hydrophila* group, respectively. The crabs were kept in aerated water and six crabs were sampled randomly at 0, 3, 6, 12, 24 and 48 h from each group after the injections, respectively. The hemolymph was collected from the last pair of walking legs from each crab by using a syringe, mixed with an equal volume of anticoagulant solution (510 mM NaCl, 100 mM glucose, 200 mM citric acid, 30 mM sodium citrate, 10 mM EDTA·2Na, pH 7.3), and centrifuged immediately at 800 *g*, 4 °C for 10 min to harvest the hemocytes. In addition, the tissues including hepatopancreas, gill, stomach, muscle, brain and hemocytes were collected from another six adult crabs. Tissues from two crabs were mixed as one sample, and there were three replicates. All these samples were preserved in 1 mL Trizol reagent (Invitrogen), frozen in liquid nitrogen, and stored at −80 °C for the subsequent RNA extraction.

2.2. RNA extraction and cDNA synthesis

Trizol reagent was used to extract the total RNA from tissue samples according to previous report [31]. The RNase-free DNase I (Takara, Japan) was used to digest the genomic DNA from the total RNA. Integrities of representative RNA samples were visualized via agarose gel electrophoresis assays. The quality and concentration of total RNA were estimated using a NanoDrop 2000 Spectrophotometer (Thermo Fisher Scientific, Wilmington, DE, USA). Only the RNA samples with an A260/A280 ratio between 1.8 and 2.0 were used for the subsequent analysis. Total RNA (1 μg) was reverse transcribed using the PrimeScript™ real-time PCR kit (Takara, Japan) for quantitative real-time PCR (qRT-PCR) analysis. The obtained cDNA was stored at −80 °C for the subsequent experiments.

2.3. Cloning and sequence analysis of full length cDNA

Bioinformatic screening of Beclin-1 gene was conducted using BLASTP (http://blast.ncbi.nlm.nih.gov/Blast.cgi) in genome database (PRJNA305216) of *E. sinensis* [32]. A Beclin-1 gene was identified from the genome database and designated as *Es*Beclin-1. A pair of gene specific primers, *Es*Beclin-1-F and -R (Table 1), was designed to amplify the open reading frame (ORF) of *Es*Beclin-1. After gel-purification with MiniBest Agarose Gel DNA Extraction Kit Ver.4.0 (Takara, Japan), the products were cloned into pMD19-T vector and sequenced in both directions with M13–47 and M13-RV (Table 1). The sequencing results were verified and subjected to cluster analysis.

2.4. Sequence analysis of EsBeclin-1

The cDNA sequence and deduced amino acid sequence of *Es*Beclin-1 were analyzed using BLAST algorithm (http://www.ncbi.nlm.nih.gov/blast) and Expert Protein Analysis System (ExPASy) (http://www.expasy.org), respectively. The protein domain was predicted with Simple Modular Architecture Research Tool (SMART) (http://smart.embl-heidelberg.de/). The coiled-coil regions were deduced using COILS software (www.embnet.vital-it.ch/software/COILS_form). The multiple sequence alignment was created using Clustal W multiple alignment program (http://www.ebi.ac.uk/clustalw/). The MEGA 6.0 package was used to construct a neighbor-joining phylogenetic tree based on the deduced amino acid sequences of *Es*Beclin-1 and other Beclin sequences. The reliability of the branching was tested by bootstrap resampling (1,000 pseudo-replicates). The presumed tertiary structures of the *C*-terminal region of Beclins were established using SWISS-MODEL prediction algorithm (http://swissmodel.expasy.org/) and displayed by Deep View/Swiss Viewer Version.

2.5. qRT-PCR analysis of EsBeclin-1 mRNA expression

qRT-PCR reactions were performed with the SYBR premix ExTap

Table 1
Primers used in this study.

Primer name	Sequence (5′-3′)
*Es*Beclin-1-F	CCATCATGGATCCACGCATA
*Es*Beclin-1-R	CTAGCTAGTGTCTCCTGGGGTGA
M13-47	CGCCAGGGTTTTCCCAGTCACGAC
M13-RV	GAGCGGATAACAATTTCACACAGG
*Es*Beclin-1-*Nde* I-F	GGGAATTCCATATGATGGATCCACGCATAACA GTCA
*Es*Beclin-1-*Xho* I-R	CCGCTCGAGGCTAGTGTCTCCTGGGGTGAT
*Es*Beclin-1-RNAi-F	TAATACGACTCACTATAGGGACGCATAACAGT CAACTTCACAT
*Es*Beclin-1-RNAi-R	TAATACGACTCACTATAGGGGAGCAAGGGATG CCAAGA
EGFP-RNAi-F	TAATACGACTCACTATAGGGCGACGTAAACGG CCACAAGT
EGFP-RNAi-R	TAATACGACTCACTATAGGGCTTGTACAGCTCG TCCATGC
*Es*Beclin-1-RT-F	TGGCATTCAGGACATTTTGGGA
*Es*Beclin-1-RT-R	CCAGACCCATACAAAGGCAGC
*Es*ALF2-RT-F	GACCCTTTGCTGAATGCTTGA
*Es*ALF2-RT-R	CTGCTCTACAATGTCGCCTGA
*Es*Crus-RT-F	GCTCTATGGCGGAGGATGTCA
*Es*Crus-RT-R	CGGGCTTCAGACCCACTTTAC
*Es*Crus2-RT-F	ACCTATGGCTGCCGCTAC
*Es*Crus2-RT-R	CAAGCGTCACAGCAGCAC
*Es*LYZ-RT-F	GCTGACTGGACCTGTAACGA
*Es*LYZ-RT-R	GCACTTCTCCACATCATCCC
*Es*β-actin-RT-F	GCATCCACGAGACCACTTACA
*Es*β-actin-RT-R	CTCCTGCTTGCTGATCCACATC

(RR420, Takara, Japan) on ABI PRISM 7500 Sequence Detection System (Thermo Fisher, USA) to examine the relative mRNA expression of *Es*Beclin-1. A pair of gene specific primers, *Es*Beclin-1-RT-F and -R (Table 1), was used to amplify a 234 bp fragment of *Es*Beclin-1. A 267 bp fragment of *Es*β-actin (GenBank accession No. HM053699) amplified with specific primers, *Es*β-actin-RT-F and -R (Table 1), was employed as endogenous control. qRT-PCR was programmed at 95 °C for 10 min, followed with 40 cycles at 95 °C for 10 s and 60 °C for 45 s. Dissociation curve analysis of amplification products was performed at the end of each PCR to confirm the specificity of PCR products. The relative mRNA expression level of *Es*Beclin-1 was analyzed by comparative Ct method ($2^{-\triangle\triangle Ct}$ method) [33].

2.6. Recombinant and purification of EsBeclin-1

The complete cDNA fragment encoding the polypeptide of *Es*Beclin-1 was amplified with specific primers *Es*Beclin-1-*Nde* I and -*Xho* I (Table 1), which contained *Nde* I and *Xho* I cleavage site sequences at the 5' end, respectively. *Nde* I and *Xho* I restriction enzymes were employed to digest PCR products. The targeted fragments were inserted into the expression vector pET-22b (Novagen, Malaysia) by T4 ligase (NEB, USA) and transformed into *E. coli* trans 5α competent cells. The recombinant plasmids of pET-22b-*Es*Beclin-1 were extracted and then transformed into *E. coli* BL21 (DE3) Chemically Competent Cell (Trans Gen Biotech, China). After screening, the positive transformants were incubated in LB medium containing 100 μg mL^{-1} ampicillin at 37 °C with shaking at 200 rpm for about 4 h. When the OD_{600} value of the culture medium reached 0.4–0.6, Isopropyl β-D-1-Thiogalactopyranoside (IPTG) was added into the LB medium at a final concentration of 1 mM and incubated under the same condition for another 5 h. The bacteria were harvested by centrifuging at 10,000 *g* for 5 min and the recombinant *Es*Beclin-1 protein (r*Es*Beclin-1) was purified by Ni-NTA sepharose column according to the previous description [34]. The purified protein was confirmed by 12% SDS-polyacrylamide gel electrophoresis (SDS-PAGE), and visualized with coomassie bright blue R250. The concentration of purified r*Es*Beclin-1 was quantified with BCA method [35]. The purified r*Es*Beclin-1 was stored at −80 °C for the preparation of polyclonal antibody.

2.7. Preparation of polyclonal antibody and western blot analysis

Polyclonal antibody against *Es*Beclin-1 were prepared with six-week-old female mice according to the previous description [36]. In western blot analysis, r*Es*Beclin-1 was separated by SDS-PAGE and transferred from gel onto nitrocellulose membrane. After washing with TBS (20 mM Tris-HCl, 150 mM NaCl, pH 8.0) and TBS-T (TBS with 0.05% Tween-20), the membrane was soaked in blocking buffer with 5% no-fat milk at 37 °C for 2 h. Then, the membrane was incubated with prepared *anti-Es*Beclin-1 antibody (pre-immune serum was used as negative control) at a ratio of 1:1,000 (v/v) at 37 °C for 1 h, and followed with extensive washing in TBS-T for three times. Next, the membrane was incubated with goat anti-mouse IgG conjugated with HRP label at a ratio of 1:2,000 (v/v) for 1 h. After a final three times of washing, the membrane was incubated in western lighting ECL substrate system (Thermo Scientific, USA) in dark for 2 min, and the immune-blotted protein bands were visualized using chemiluminescent imaging system (Amersham Imager 600, USA).

2.8. Immunofluorescence assay of EsBeclin-1 in E. sinensis hemocytes

Immunofluorescence assay of *Es*Beclin-1 from hemocytes after LPS stimulation was performed according to the previous report with some modifications [34]. Briefly, hemocytes were collected at 2 h after LPS or PBS injections, and fixed with 4% paraformaldehyde for 20 min. After washing with PBS for three times, the hemocytes were resuspended in L15 cell culture media and deposited on dishes pre-coated with poly-L-lysine and incubated at room temperature for 3 h to adhere to the wall. The samples were permeabilized with 0.5% (v/v) Triton X-100 for 15 min, and then washed with PBS-T (PBS with 0.1% Tween-20). The hemocytes were blocked with 3% (w/v) Fetal bovine serum albumin diluted in PBS-T at room temperature for 1 h and then incubated with 100 μL *anti-Es*Beclin-1 antibody or non-immunized mouse serum (diluted 1:500 (v/v) in blocking buffer) at 37 °C for 1 h. After washing, the samples were incubated with Alexa Fluor 488-labeled goat-*anti*-mouse antibody (diluted 1:1,000 (v/v) in blocking buffer) at 37 °C for 50 min. A volume of 50 μL 4, 6-diamidino-2-phenylindole hydrochloride (DAPI, diluted 1:1,000 with blocking buffer) was added to stain the nucleus for 15 min. After the final three times of washing, coverslips were fixed on slides containing a volume of 20 μL fluorescent mounting media. The crab hemocytes were observed by using Carl Zeiss Axio Imager A2 microscope (Carl Zeiss, Germany).

2.9. RNA interference assay

The double strands RNA (dsRNA) of *Es*Beclin-1 was synthesized according to the method described in previous report [31]. T7 promoter linked primers, *Es*Beclin-1-RNAi-F and -R, EGFP-RNAi-F and -R (Table 1), were used to amplify the DNA fragment of *Es*Beclin-1 (857 bp) from crab genomic DNA and enhanced green fluorescent protein (EGFP) DNA (657 bp) from pEGFP vector, respectively. The amplified DNA products were used as templates to synthesize dsRNA, and the dsRNAs of *Es*Beclin-1 and EGFP were dissolved in PBS at a final concentration of 1 μg $μL^{-1}$. Forty-eight crabs were employed for the RNA interference experiment. The crabs were randomly divided into four groups (Blank group, PBS group, dsEGFP group, and ds*Es*Beclin-1 group). Crabs in PBS group, dsEGFP group and ds*Es*Beclin-1 group received an injection of 100 μL PBS, EGFP-dsRNA, and *Es*Beclin-1-dsRNA, respectively. The untreated crabs were used as blank controls. Six crabs in each group were randomly sampled at 0 and 24 h post injections, respectively. The RNA-interfered crabs were further stimulated with LPS. Twenty four crabs were randomly arranged into four groups, including PBS + PBS group, PBS + LPS group, dsEGFP + LPS group, and ds*Es*Beclin-1 + LPS group. The crabs in PBS + LPS group, dsEGFP + LPS group and ds*Es*Beclin-1 + LPS group received an injection of 100 μL LPS at 24 h after PBS or dsRNA injecting, while the PBS + PBS

group received an injection of 100 μL PBS at 24 h after PBS injecting. Six crabs from each group were sampled at 6 h after the second injections, respectively. The collection of hemocytes, RNA extraction and cDNA synthesis were conducted as the method mentioned above. The RNAi efficiency was assessed by qRT-PCR reactions on ABI PRISM 7500 Sequence Detection System (Thermo Fisher, USA) with primers *Es*Beclin-1-RT-F and -R (Table 1). The mRNA expressions of AMPs (*Es*ALF2, GenBank accession No. GU014699.1; *Es*LYZ, GenBank accession No. AEU04535.1; *Es*Crus, GenBank accession No. GQ200832; *Es*Crus2, GenBank accession No. GQ200833.1) were detected by qRT-PCR with gene specific primers (Table 1).

2.10. Statistical analysis

All data represented as mean ± S.E. (N = 3) were analyzed and graphed using Statistical Package for Social Sciences (SPSS) 22.0 and Origin 8.1 (Origin Lab, Northampton, MA, USA), respectively. A multiple comparison (Duncan) test was carried out to examine the significant differences among different groups. Significant differences across controls were indicated with an asterisk at $p < 0.05$, and with two asterisks at $p < 0.01$.

3. Results

3.1. Identification and characterization of EsBeclin-1

A novel Beclin-1 gene was identified from *E. sinensis*, which was deposited in GenBank under accession No. MH173046. The ORF of *Es*Beclin-1 was of 1,275 bp, encoding a polypeptide of 424 amino acids (Fig. 1A). The predicted molecular weight and theoretical isoelectric point of *Es*Beclin-1 were 48.5 kDa and 5.1, respectively. A typical APG6 domain (from Pro105 to Leu415) and an *N*-terminal low complexity region were identified in *Es*Beclin-1 by SMART analysis (Fig. 1B). The deduced amino acid sequence of *Es*Beclin-1 shared high similarity ranging from 42.9% to 63.6% with that of other previously identified Beclin proteins (Fig. 2), including *Dm*Atg6 from fruit fly *Drosophila melanogaster* (63.6%), *Mm*Beclin-1 from mouse *Mus musculus* (56.6%), *Bt*Beclin-1 from holstein *Bos taurus* (56.3%), *Xt*Beclin-1 from clawed frog *Xenopus tropicalis* (56.2%), *Hs*Beclin-1 from human *Homo sapiens* (56.0%), *Dr*Beclin-1 from zebrafish *Danio rerio* (55.8%), *Hs*Beclin-2 from *H. sapiens* (46.2%), and *Mm*Beclin-2 from *M. musculus* (42.9%). *Es*Beclin-1 also possessed a conserved ECD domain (Asp215 to Ser307) and a CCD domain (Val147 to Cys204) (Fig. 2). Though there was no definite BH3 domain in *Es*Beclin-1, several key residues (Leu86, Lys87 and Phe93) were found similar to those in human BH3 domain (Fig. 2).

A phylogenetic tree was constructed based on the amino acid sequences of 19 Beclin orthologous genes by the neighbor-joining method (Fig. 3). All the selected Beclin genes from vertebrates and invertebrates were separated clearly into Beclin-1 and Beclin-2 branches, and Beclin-1s from vertebrates and invertebrates were assigned into two independent sub-branches. *Es*Beclin-1 was firstly clustered with Atg6 from *D. melanogaster* and then assigned into the sub-branch of invertebrate Beclin-1. The potential tertiary structures of the *C*-terminal regions of *Hs*Beclin-1 (Fig. 4A), *Hs*Beclin-2 (Fig. 4B), *Dm*Atg6 (Fig. 4C) and *Es*Beclin-1 (Fig. 4D) were established using the SWISS-MODEL prediction algorithm based on the template 4ddp.1.A. Multiple alignment analysis revealed that the conserved ECD was located at the *C*-terminus of *Es*Beclin-1. The *C*-terminal region of *Es*Beclin-1 showed high similarity with that of *Hs*Beclin-1 (72.9%) and *Dm*Atg6 (75.9%), while low with that of *Hs*Beclin-2 (55.2%) (data not shown). The *C*-

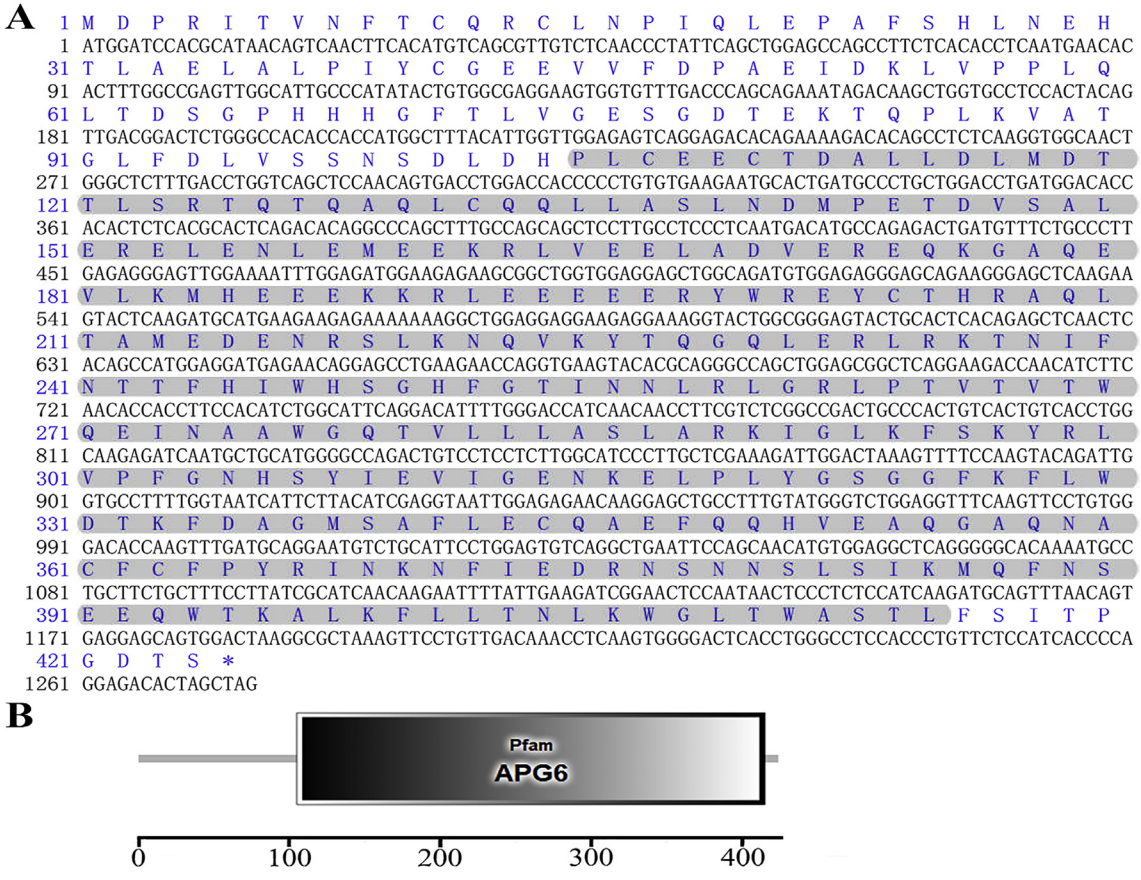

Fig. 1. Nucleotide, deduced amino acid sequence and protein domain of *Es*Beclin-1. A: The nucleotide and amino acids are numbered along the left margin. The star (*) indicates the stop cordon. APG6 domain is shadowed in gray. B: Conserved protein domain of *Es*Beclin-1 is predicted by SMART (http://smart.embl.de/). There is a low complexity region and a typical APG6 domain in *Es*Beclin-1.

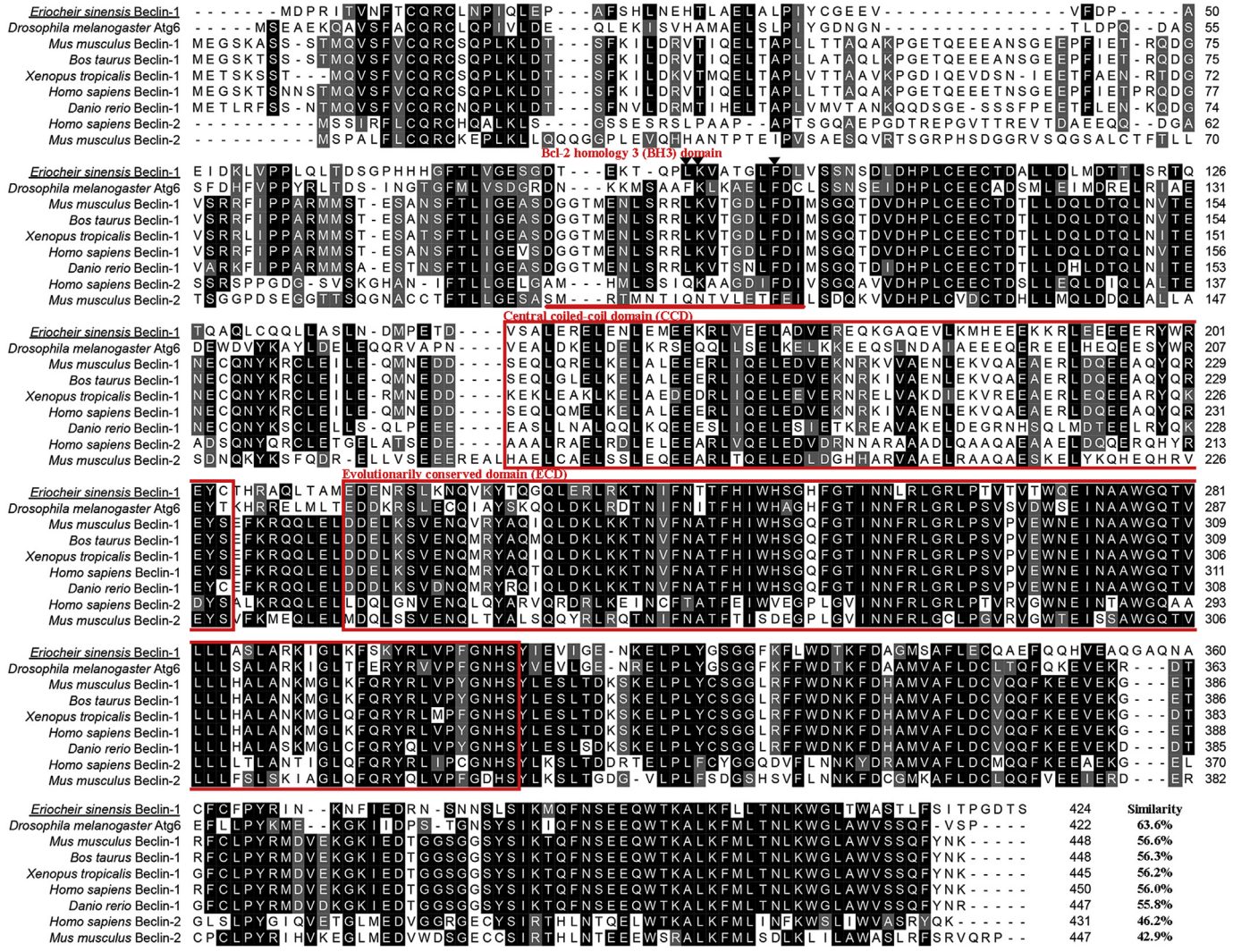

Fig. 2. Sequence characteristics of *Es*Beclin-1. Multiple sequence alignment of *Es*Beclin-1 with other Beclin protein sequences is built by Clustal W. The species and the GenBank accession numbers are as follows: autophagy-related gene 6 from fruit fly *Drosophila melanogaster* (NP_651209.1); Beclin-1 from mouse *Mus musculus* (NP_062530.2), holstein *Bos taurus* (NP_001028799.1), clawed frog *Xenopus tropicalis* (CAJ19734.1), human *Homo sapiens* (NP_001300927.1), and zebrafish *Danio rerio* (NP_957166.1); Beclin-2 from *H. sapiens* (NP_001277622.1), and *M. musculus* (NP_001277621.1). *Es*Beclin-1 is underlined. The shaded regions indicate the identical residues. Other conserved, but not consensus amino acids, are shaded in gray (similarity > 60%). The central coiled coil domain (CCD, residues 147–204) and evolutionarily conserved domain (ECD, residues 215–307) of *Es*Beclin-1 are boxed with red lines, respectively. The BH3 domain in human is underlined with a red line. The conserved key residues in BH3 are marked with (▼) (Leu86, Lys87 and Phe93 in *E. seninsis*). Gaps are indicated by dashes to improve the alignment. (For interpretation of the references to color in this figure legend, the reader is referred to the Web version of this article.)

terminal region of *Es*Beclin-1 contained three internal repeats and each contained an ensuing α-helix and a pair of short β-strands. The three α-helices (α2, α3, and α4) formed a parallel bundle at the center, surrounded by three β-sheets, six loops, and the *N*-terminal α1 helix. A prominent feature of the structure was protrusion of loop away from the main ellipsoid. Three aromatic amino acids were located at the tip of the protrusion in *Hs*Beclin-1, *Dm*Atg6 and *Es*Beclin-1, whereas none was in *Hs*Beclin-2.

3.2. Tissue distribution of *Es*Beclin-1 mRNA

The mRNA transcripts of *Es*Beclin-1 in different tissues including hepatopancreas, gill, stomach, muscle, brain and hemocytes were detected by qRT-PCR (Fig. 5). The highest mRNA expression level of *Es*Beclin-1 was detected in hepatopancreas, which was 14.74-fold ($p < 0.01$) of that in stomach. The relative mRNA expression levels of *Es*Beclin-1 in hemocytes, gill, brain and muscle were 8.94-fold ($p < 0.01$), 5.56-fold ($p < 0.01$), 1.97-fold ($p > 0.05$) and 1.27-fold ($p > 0.05$) of that in stomach, respectively.

3.3. The temporal mRNA expression pattern of *Es*Beclin-1 after LPS and *A. hydrophila* stimulations

The mRNA transcripts of *Es*Beclin-1 in hemocytes after LPS and *A. hydrophila* stimulations were detected by qRT-PCR with *Es*β-actin as internal control. The *Es*Beclin-1 mRNA in hemocytes was significantly enhanced after LPS and *A. hydrophila* stimulations. After LPS stimulation (Fig. 6A), the mRNA expression level of *Es*Beclin-1 was significantly up-regulated at 3 h (2.94-fold, $p < 0.01$), reached the highest level at 6 h (4.70-fold, $p < 0.01$), kept the significantly high level (2.5-fold, $p < 0.01$) until 24 h, and then down-regulated to 1.30-fold ($p > 0.05$) at 48 h. Upon *A. hydrophila* stimulation (Fig. 6B), the mRNA transcripts of *Es*Beclin-1 were significantly increased during the early stage. Its expression level rose strikingly from 3 to 12 h with the maximum level of 2.91-fold ($p < 0.01$) at 6 h compared to that in the control group, and declined to 1.64-fold ($p > 0.05$) at 24 h. In the

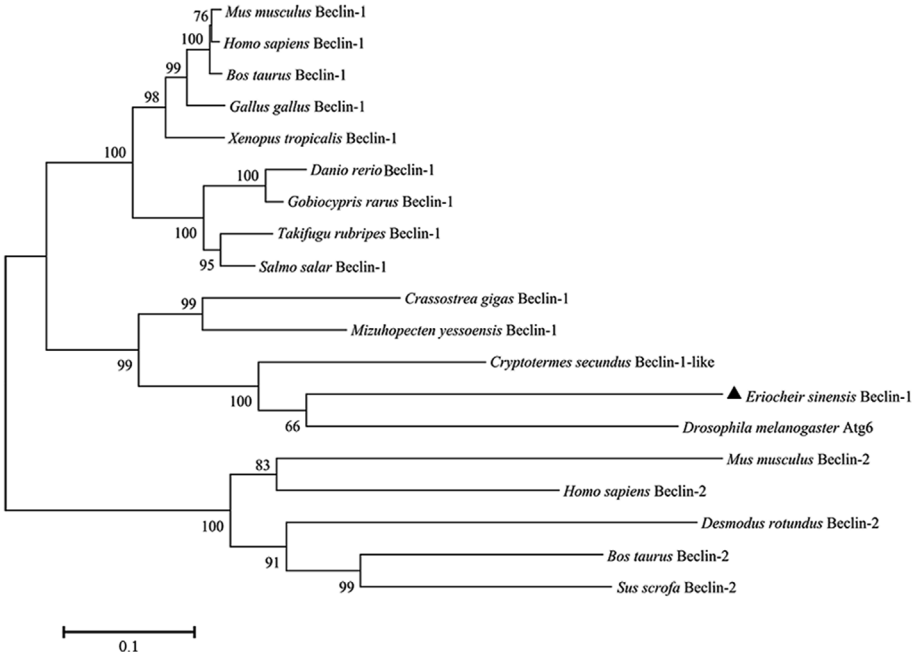

Fig. 3. The phylogenetic tree of Beclins from invertebrates and vertebrates. Sequence alignment is created using the MEGA 6.0 based on the amino acid sequences of 19 Beclin family members from different species. The phylogenetic tree is built by neighbor-joining algorithm, and bootstrap resampling (1,000 pseudo-replicates) is used to test the reliability of the branching. The organisms and the GenBank accession numbers are as follows: Beclin-1 from *H. sapiens*, *M. musculus*, *B. taurus*, *X. tropicalis*, *D. rerio*, *Gallus gallus* (NP_001006332.1), *Gobiocypris rarus* (AJP31411.1), *Takifugu rubripes* (NP_001032963.1), *Salmo salar* (NP_001133290.1), *Crassostrea gigas* (EKC28450.1), and *Mizuhopecten yessoensis* (OWF44040.1), Beclin-1 like from *Cryptotermes secundus* (PNF22772.1), Atg6 from *D. melanogaster*, Beclin-2 from *H. sapiens*, *M. musculus*, *Desmodus rotundus* (XP_024431741.1), *B. Taurus* (XP_003587111.1), and *Sus scrofa* (XP_003130605.1).

control group, no prominent changes were observed during the whole period of PBS stimulation.

3.4. Recombinant protein of EsBeclin-1 and specificity of its polyclonal antibody

r*Es*Beclin-1 was purified by Ni-NATA affinity chromatography and confirmed by 12% SDS-PAGE. A distinct band with a molecular weight about 49 kDa was observed in SDS-PAGE (lane 3 in Fig. 7A), which was consistent with the predicted molecular mass of *Es*Beclin-1. The purified r*Es*Beclin-1 was employed to prepare polyclonal antibody. The specificity of *anti-Es*Beclin-1 polyclonal antibody was detected by western blot. A clear reaction band about 49 kDa with high specificity was revealed (lane 1 in Fig. 7B), which corresponded exactly to the molecular mass of r*Es*Beclin-1. As negative control, no visible band was detected in the group of the mouse pre-immune serum (lane 2 in Fig. 7B).

3.5. Subcellular localization of EsBeclin-1 in E. sinensis hemocytes

Immunofluorescence assay was performed to explore the subcellular localization of *Es*Beclin-1 protein in *E. sinensis* hemocytes at 2 h after LPS or PBS stimulations (Fig. 8). In the bright field, the hemocytes were observed in irregular shapes. The nucleus stained by DAPI was observed in blue, and the *Es*Beclin-1-immunoreactive areas were shown in green. According to the merged images, the positive green signals showed diffuse localization in the cytoplasm after PBS injection, whereas they

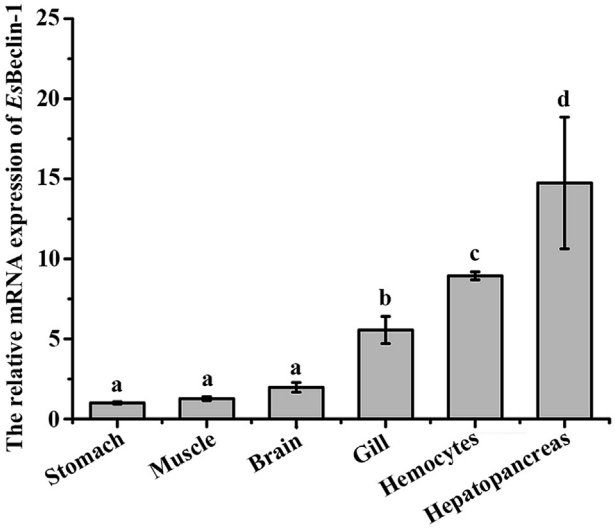

Fig. 5. The relative mRNA expression of *Es*Beclin-1 in different tissues of *E. sinensis*. Comparison of the mRNA expression level of *Es*Becin-1 (relative to *Es*β-actin) among different tissues is normalized to stomach. Vertical bars represent the mean ± S.D. (N = 3) for each tissue. The different letters show that there exist significant differences comparing with other groups ($p < 0.05$, ANOVA).

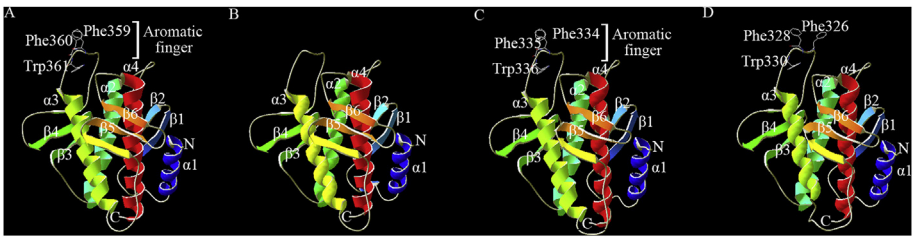

Fig. 4. The spatial structures of the *C*-terminal regions in *Hs*Beclin-1, *Hs*Beclin-2, *Dm*Atg6 and *Es*Beclin-1 are predicted by SWISS-MODEL program based on the template 4ddp.1.A. A: Overall structure of the *C*-terminal region (residues 248–447) of *Hs*Beclin-1. B: Overall structure of the *C*-terminal region (residues 230–429) of *Hs*Beclin-2. C: Overall structure of the *C*-terminal region (residues 224–419) of *Dm*Atg6. D: Overall structure of the *C*-terminal region (residues 218–416) of *Es*Beclin-1. The *C*-terminal region is composed of three structural repeats containing a pair of β-strands and a long α-helix. The structures are shown in rainbow color, with the *N*- and *C*-termini colored blue and red, respectively. There is an aromatic finger protruded from the core structure in A and C. A similar structure of the aromatic finger is protruded from the core structure in D. (For interpretation of the references to color in this figure legend, the reader is referred to the Web version of this article.)

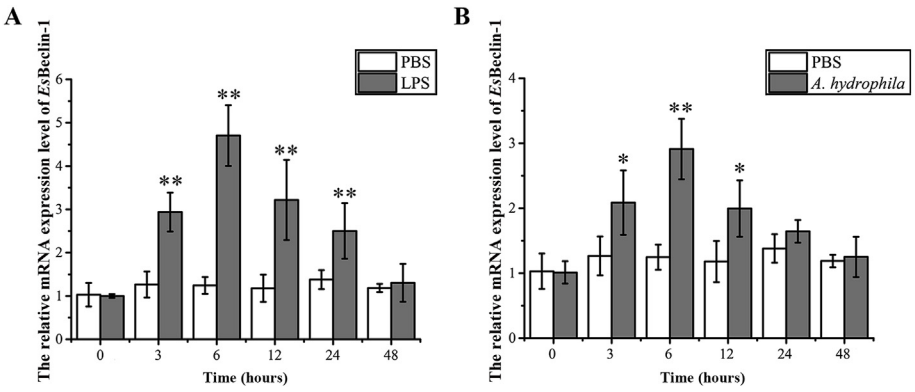

Fig. 6. The temporal mRNA expression of *Es*Beclin-1 after immune stimulations in hemocytes of *E. sinensis*. A: The temporal expression of *Es*Beclin-1 at 0, 3, 6, 12, 24 and 48 h after LPS stimulation with PBS as control. B: The temporal expression of *Es*Beclin-1 at 0, 3, 6, 12, 24 and 48 h after *A. hydrophila* stimulation with PBS as control. Comparison of the mRNA expression level of *Es*Beclin-1 (relative to *Es*β-actin) is normalized to 0 h. Vertical bars represent the mean ± S.D. (N = 3). One asterisk indicates significant difference at $p < 0.05$, and two asterisks indicates extremely significant difference at $p < 0.01$.

were predominantly aggregated and punctuated in the cytoplasm upon LPS stimulation. No visiblly positive signal was observed in the negative control.

3.6. The mRNA expressions of AMPs after the inhibition of EsBeclin-1

The double strands RNA interference strategy was employed to interfere the expression of *Es*Beclin-1. LPS stimulation was carried out in *Es*Beclin-1-interfered crabs as mentioned above and qRT-PCR was used to detect the mRNA expressions of *Es*Beclin-1 and *E. sinensis* AMPs in hemocytes. The relative mRNA expression of *Es*Beclin-1 was significantly decreased at 24 h post the injection of *Es*Beclin-1-dsRNA, which was about 0.27-fold ($p < 0.01$) of that in the dsEGFP group (Fig. 9A). No significant changes were observed in PBS group (0.92-fold, $p > 0.05$) and dsEGFP group (1.03-fold, $p > 0.05$) compared with that in the Blank group. To further explore the involvement of *Es*Beclin-1 in regulating AMPs, the mRNA expressions of AMPs (*Es*ALF2, *Es*LYZ, *Es*Crus and *Es*Crus2) were examined at 6 h after LPS stimulation in *Es*Beclin-1-interfered crabs. The mRNA transcripts of *Es*ALF2 (Fig. 9B) declined significantly to 0.55-fold ($p < 0.05$) of that in the dsEGFP + LPS group. Additionally, the mRNA reductions of *Es*LYZ (Fig. 9C), *Es*Crus (Fig. 9D) and *Es*Crus2 (Fig. 9E) were extremely significant, which were 0.21-fold ($p < 0.01$), 0.49-fold ($p < 0.01$) and 0.46-fold ($p < 0.01$), compared to that in the dsEGFP + LPS group, respectively. No significant changes were observed between PBS + LPS group and dsEGFP + LPS group.

4. Discussion

As a key regulator in autophagy initiation and autophagosomes maturation, Beclin-1 has aroused wide attentions. It has been identified to be involved in various biological processes, including development, tumor suppression, and lifespan extension [7,8]. Increasing evidences have also demonstrated that Beclin-1 plays an important role in immune responses in many species [22,23,37]. In the present study, a novel homolog of Beclin-1, *Es*Beclin-1, was identified from *E. sinensis*. A conserved APG6 domain was identified in *Es*Beclin-1, suggesting that *Es*Beclin-1 was a typical member of Beclin family [38,39]. Meanwhile, a conserved ECD and a CCD were also identified in the region of APG6 domain in *Es*Beclin-1. The ECD domain of *Es*Beclin-1 shared high similarity with that in other species, which might endow *Es*Beclin-1 with the possible function to interact with PI3K and participate in autophagy initiation and autophagosomes maturation [4,7,14]. No typical BH3 domain was identified in *Es*Beclin-1, which was different from the most Beclin-1s [10]. Although the BH3 domain was not clearly identified in APG6 domain, the key residues of BH3 essential for its interaction with Bcl-XL or Bcl-2 in human were found in *Es*Beclin-1 (Leu86, Lys87 and Phe93) [40], indicating that *Es*Beclin-1 might probably interact with Bcl-2 through these residues. The high similarities and conserved functional domains of *Es*Beclin-1 further suggested that *Es*Beclin-1 was a member of the Beclin family.

A phylogenetic tree was constructed based on the amino acid sequences of 19 selected Beclin orthologous genes. There were two distinct branches in the tree, including Beclin-1/Atg6 from vertebrates and invertebrates as well as the mammalian-specific Beclin-2. *Es*Beclin-1 was firstly grouped with invertebratesBeclin-1s as a separate clade, and then clustered with Beclin-1s from vertebrates. The amino acid sequence of *Es*Beclin-1 shared higher sequence similarity with Beclin-1 (55.8–63.6%) than Beclin-2 (46.2–46.9%). In addition, the spatial structure of *C*-terminal region of *Es*Beclin-1 predicted with SWISS-MODEL prediction algorithm was a compact ellipsoid consisted of three β-sheet-α-helix repeats, which was similar to other known Beclin-1s [10,13]. The *C*-terminal region of *Es*Beclin-1 shared higher similarity with that of human Beclin-1 and fly Atg6 than that of human Beclin-2. Strikingly, three incoherent aromatic amino acids (Phe326, Phe328 and Trp330) were found to be located at the tip of the protrusion of loop in *Es*Beclin-1, which was similar to that in the corresponding region of *Hs*Beclin-1 and *Dm*Atg6 [10]. As the aromatic finger of *Hs*Beclin-1 was reported to be needed for the membrane association [10], it was suspected that the aromatic amino acids in *Es*Beclin-1 might be required in membrane association. The phylogenetic relationship and spatial structure further suggested that *Es*Beclin-1 was a conserved member of Beclin-1 subfamily.

Beclin-1 had been identified from many species, and it was

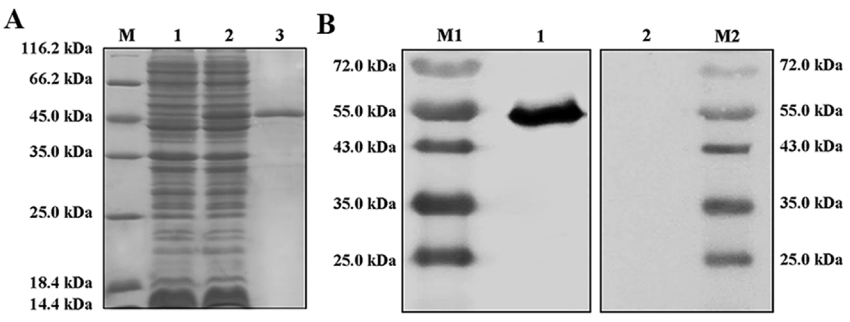

Fig. 7. SDS-PAGE and western blot analysis of *Es*Beclin-1. A: Lane M: standard protein molecular weight marker; Lane 1: negative control for r*Es*Beclin-1 (without IPTG induction); Lane 2: IPTG induced r*Es*Beclin-1 (the whole cell lysate); Lane 3: purified r*Es*Beclin-1 protein. B: Lane M1: standard protein molecular weight marker; Lane 1: western blot analysis of r*Es*Beclin-1 with prepared *anti-Es*Beclin-1 antibody; Lane 2: western blot analysis of r*Es*Beclin-1 with pre-immune serum from mice; Lane M2: standard protein molecular weight marker.

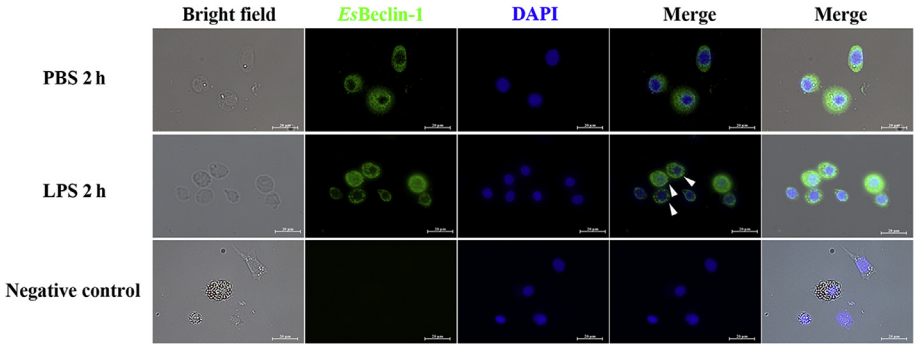

Fig. 8. Subcellular localization of *Es*Beclin-1 in hemocytes. The morphology of hemocytes is shown in bright field. Positive signals of *Es*Beclin-1 are shown in green and the nucleus stained by DAPI is shown in blue. (For interpretation of the references to color in this figure legend, the reader is referred to the Web version of this article.)

characterized to be involved in diverse biological processes. The distribution of *Es*Beclin-1 in different tissues and the subcellular localization of *Es*Beclin-1 protein in hemocytes were investigated to understand its potential function in crustaceans. The *Es*Beclin-1 mRNA could be detected in all examined tissues, which was similar to the reports in other species. For example, the mRNA transcripts of Beclin-1 and Beclin-2 were extensively detected in various tissues of human and mouse [6]. In *C. semilaevis*, *Cs*Beclin-1 was expressed in various tissues, especially with higher expression level in blood [23]. The constitutive distributions of *Es*Beclin-1 mRNA indicated its potentially diversified functions. The expression level of *Es*Beclin-1 mRNA was obviously higher in hepatopancreas and hemocytes, which were considered to play key roles in metabolism and innate immunity in crustaceans [41,42]. Immunofluorescence assay indicated that *Es*Beclin-1 protein was mainly distributed in the cytoplasm of hemocytes. It was reported that *Mm*Beclin-1 displayed a diffuse distribution in the cytoplasm of various tissues in mice [43], and Beclin-1 in HeLa cells showed profoundly cytoplasmic punctuate staining upon stimulation with herring testis DNA, immune stimulatory DNA or herpes simplex virus-1 infection [22]. In the present study, the *Es*Beclin-1 protein also aggregated and displayed predominantly cytoplasmic punctuate staining in a portion of hemocytes at 2 h after LPS stimulation. Given that LPS could induce considerable autophagy and immune responses in immune cells [44], all these results indicated that *Es*Beclin-1 might participate in immune responses in *E. sinensis*.

For further understanding the function of *Es*Beclin-1 in the immune system, the mRNA expression of *Es*Beclin-1 in hemocytes of *E. sinensis* post immune stimulations was explored by qRT-PCR. The relative mRNA expression of *Es*Beclin-1 in hemocytes was significantly up-regulated at 3, 6 and 12 h after LPS and *A. hydrophila* stimulations. Similarly, the expression of *Cs*Beclin-1 in *C. semilaevis* increased significantly in head kidney in response to *Edwardsiella tarda* and *Vibrio harveyi* stimulations [23]. It was reported that LPS could induce autophagy through Beclin-1 in human peritoneal mesothelial cell line, and the activation of Toll-like receptor 4 (TLR4) signaling pathway was involved in autophagy [45]. TLR pathways are crucial in recognizing LPS and triggering downstream humoral and cellular immune responses in crustacean [46]. These results suggested that LPS could induce the mRNA expression of Beclin-1 and autophagy through TLR signaling pathways. The up-regulation of *Es*Beclin-1 transcripts after immune stimulations indicated that *Es*Beclin-1 might play an important role in the innate immune responses against the invading microbial pathogens in *E. sinensis*.

It was previously reported that Beclin-1 could interact with the catalytic subunits of IKK through its *C*-terminal 150 amino acids and regulate the activity of NF-κB in mammals [27]. In the present study, the *C*-terminal region of *Es*Beclin-1 was found to share high similarity with that of human Beclin-1 and flies Atg6, which might provide *Es*Beclin-1 the possibility to interact with IKK and stimulate the downstream immune responses. IKK has been identified to play crucial roles in the activation of NF-κB from invertebrates to vertebrates [47,48]. Both *Lv*IKKβ and *Lv*IKKε from *L. vannamei* could activate NF-κB receptor in HEK293T cells to regulate AMPs expression [49]. In the present study, dsRNAi strategy was employed to inhibit the expression

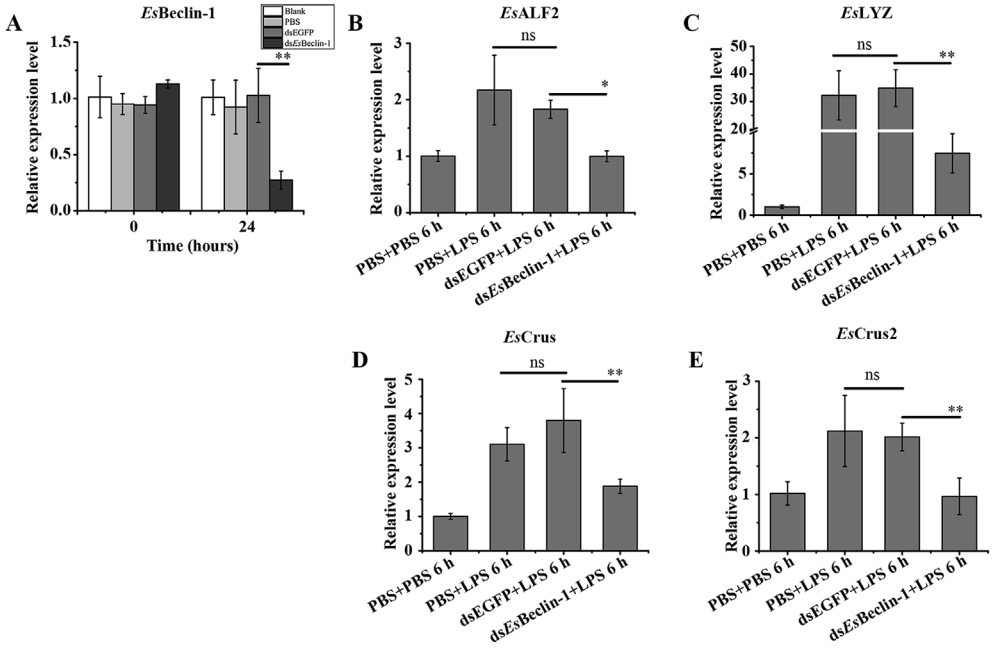

Fig. 9. The mRNA expressions of AMPs (*Es*ALF2, *Es*LYZ, *Es*Crus and *Es*Crus2) after LPS stimulation in hemocytes in *Es*Beclin-1-interfered crabs. A: The efficiency of *Es*Beclin-1 inhibition. B–E: The mRNA expression level of *Es*ALF2, *Es*LYZ, *Es*Crus and *Es*Crus2 after LPS stimulation in ds*Es*Beclin-1-injection crabs with dsEGFP + LPS group as the control. Vertical bars represent the mean ± S.D. (N = 3). One asterisk indicates significant difference at $p < 0.05$, and two asterisks indicates extremely significant difference at $p < 0.01$, "ns" means not significant.

of *Es*Beclin-1, and the expressions of AMPs were then investigated after LPS stimulation to elucidate the potential role of *Es*Beclin-1 in regulating AMPs expression. The relative mRNA expression levels of *Es*ALF2, *Es*LYZ, *Es*Crus and *Es*Crus2 in hemocytes decreased dramatically at 6 h after LPS stimulation in *Es*Beclin-1-interfered crabs compared to that in the dsEGFP + group, indicating that *Es*Beclin-1 might participate in the regulation of these AMPs. AMPs are small cationic molecules with antibacterial activities. They are thought to be essential for organisms lacking adaptive immunity to eliminate pathogenic bacteria [50]. In shrimp, three kinds of AMPs genes, including ALFs, crustins and lysozymes were regulated by IMD pathway [51]. *Es*ALF2 from *E. sinensis* exhibited antimicrobial activity against *L. anguillarum* and *Pichia pastoris* [52]. LYZ from *L. vannamei* displayed strong antibacterial activity against gram-negative bacteria [53]. Given that the expression of *Es*Beclin-1 was significantly increased upon LPS and *A. hydrophila* stimulations, it encouraged us to suspect that *Es*Beclin-1 might participate in regulating AMPs expression to defense against bacterial challenges in *E. sinensis*.

In conclusion, a novel Beclin-1 was identified in *E. sinensis*. The *Es*Beclin-1 mRNA was constitutively expressed in all the tested tissues with higher expression level in hepatopancreas and hemocytes. *Es*Beclin-1 proteins exhibited punctuate distribution in cytoplasm of crab hemocytes under LPS stimulation. The mRNA transcripts of *Es*Beclin-1 were significantly induced by LPS and *A. hydrophila* stimulations. The mRNA expressions of *Es*ALF2, *Es*LYZ, *Es*Crus and *Es*Crus2 were all significantly decreased post LPS stimulation in *Es*Beclin-1-interfered crabs. Those results indicated that *Es*Beclin-1 might play a crucial role in immune response against bacteria through regulating the AMPs expression, which might provide new insights to better understand the function of Beclin-1 in immune responses in invertebrates.

Acknowledgement

We are grateful to all the laboratory members for their technical advice and helpful discussions. This research was supported by National key R&D Program of China (2018YFD0900606), a grant from National Science Foundation of China (No. 31530069), AoShan Talents Cultivation Program Supported by Qingdao National Laboratory for Marine Science and Technology (No. 2017ASTCP-OS13), the Outstanding Talents and Innovative teams of Agricultural Scientific Research in Ministry of Agriculture, Dalian High Level Talent Innovation Support Program (2015R020), Program for Innovative Talents in Higher Education of Liaoning Province (LR2016036), the Research Foundation for Distinguished Professor in Liaoning and Talented Scholars in Dalian Ocean University.

References

[1] D. Glick, S. Barth, K.F. Macleod, Autophagy: cellular and molecular mechanisms, J. Pathol. 221 (1) (2010) 3–12.
[2] S. Wesselborg, B. Stork, Autophagy signal transduction by ATG proteins: from hierarchies to networks, Cell. Mol. Life Sci. 72 (24) (2015) 4721–4757.
[3] B. Levine, N. Mizushima, H.W. Virgin, Autophagy in immunity and inflammation, Nature 469 (7330) (2011) 323–335.
[4] Z. Xie, D.J. Klionsky, Autophagosome formation: core machinery and adaptations, Nat. Cell Biol. 9 (2007) 1102–1109.
[5] A. Kuma, M. Komatsu, N. Mizushima, Autophagy-monitoring and autophagy-deficient mice, Autophagy 13 (10) (2017) 1619–1628.
[6] L.K. Kleeman, X.H. Liang, J.E. Goldman, G. Berry, et al., Protection against fatal sindbis virus encephalitis by Beclin, a novel Bcl-2-interacting protein, J. Virol. 72 (11) (1998) 8586–8596.
[7] C. He, B. Levine, The Beclin 1 interactome, Curr. Opin. Cell Biol. 22 (2) (2010) 140–149.
[8] Z. Yue, S. Jin, C. Yang, A.J. Levine, et al., Beclin 1, an autophagy gene essential for early embryonic development, is a haploinsufficient tumor suppressor, Proc. Natl. Acad. Sci. U. S. A. 100 (25) (2003) 15077–15082.
[9] B. Levine, R. Liu, X. Dong, Q. Zhong, Beclin orthologs: integrative hubs of cell signaling, membrane trafficking, and physiology, Trends Cell Biol. 25 (9) (2015) 533–544.
[10] W. Huang, W. Choi, W. Hu, N. Mi, et al., Crystal structure and biochemical analyses reveal Beclin 1 as a novel membrane binding protein, Cell Res. 22 (3) (2012) 473–489.
[11] S.L. Wechman, A.K. Pradhan, R. DeSalle, S.K. Das, et al., New insights into Beclin-1: evolution and pan-malignancy inhibitor activity, Adv. Cancer Res. 137 (2018) 77–114.
[12] S. Erlich, L. Mizrachy, O. Segev, L. Lindenboim, et al., Differential interactions between Beclin 1 and Bcl-2 family members, Autophagy 3 (6) (2014) 561–568.
[13] S. Suwansa-Ard, W. Kankuan, T. Thongbuakaew, J. Saetan, et al., Transcriptomic analysis of the autophagy machinery in crustaceans, BMC Genomics 17 (1) (2016) 587.
[14] J.H. Baek, J. Jung, J. Seo, J.H. Kim, et al., Bacterial overexpression and denaturing purification of VPS34-binding domain of Beclin 1, J. Microbiol. Biotechnol. 26 (10) (2016) 1808–1816.
[15] C. Liang, J.S. Lee, K.S. Inn, M.U. Gack, et al., Beclin1-binding UVRAG targets the class C Vps complex to coordinate autophagosome maturation and endocytic trafficking, Nat. Cell Biol. 10 (7) (2008) 776–787.
[16] R. Kang, H.J. Zeh, M.T. Lotze, D. Tang, The Beclin 1 network regulates autophagy and apoptosis, Cell Death Differ. 18 (4) (2011) 571–580.
[17] V.M. Aita, X.H. Liang, V.V.V.S. Murty, D.L. Pincus, et al., Cloning and genomic organization of Beclin 1, a candidate tumor suppressor gene on chromosome 17q21, Genomics 59 (1999) 59–65.
[18] Y.Y. Jung, Y.K. Lee, J.S. Koo, The potential of Beclin 1 as a therapeutic target for the treatment of breast cancer, Expert Opin. Ther. Targets 20 (2) (2016) 167–178.
[19] B.V. Shravage, J.H. Hill, C.M. Powers, L. Wu, et al., Atg6 is required for multiple vesicle trafficking pathways and hematopoiesis in *Drosophila*, Development 140 (6) (2013) 1321–1329.
[20] C. He, Y. Wei, K. Sun, B. Li, et al., Beclin 2 functions in autophagy, degradation of G protein-coupled receptors, and metabolism, Cell 154 (5) (2013) 1085–1099.
[21] A. Meléndez, Z. Tallóczy, M. Seaman, E.L. Eskelinen, et al., Autophagy genes are essential for dauer development and life-span extension in *C. elegans*, Science 301 (2003) 1387–1391.
[22] Q. Liang, G.J. Seo, Y.J. Choi, M.J. Kwak, et al., Crosstalk between the cGAS DNA sensor and Beclin-1 autophagy protein shapes innate antimicrobial immune responses, Cell Host Microbe 15 (2) (2014) 228–238.
[23] X.P. Li, H. Chi, J. Zhang, Beclin-1 is involved in tongue sole *Cynoglossus semilaevis* immune defense against bacterial infection, Fish Shellfish Immunol. 77 (2018) 8–12.
[24] K. Jia, C. Thomas, M. Akbar, Q. Sun, et al., Autophagy genes protect against *Salmonella typhimurium* infection and mediate insulin signaling-regulated pathogen resistance, Proc. Natl. Acad. Sci. U. S. A. 106 (34) (2009) 14564–14569.
[25] H.J. Kong, J.Y. Moon, B.H. Nam, Y.O. Kim, et al., Molecular characterization of the autophagy-related gene Beclin-1 from the olive flounder (*Paralichthys olivaceus*), Fish Shellfish Immunol. 31 (2) (2011) 189–195.
[26] R. Mathew, C.M. Karp, B. Beaudoin, N. Vuong, et al., Autophagy suppresses tumorigenesis through elimination of p62, Cell 137 (6) (2009) 1062–1075.
[27] L. Chen, D. Liu, Y. Zhang, H. Zhang, et al., The autophagy molecule Beclin 1 maintains persistent activity of NF-κB and Stat3 in HTLV-1-transformed T lymphocytes, Biochem. Biophys. Res. Commun. 465 (4) (2015) 739–745.
[28] M.N. Santano, A. Criollo, S.A. Malik, M. Michaud, et al., Direct molecular interactions between Beclin 1 and the canonical NF-κB activation pathway, Autophagy 8 (2) (2012) 268–270.
[29] X. Li, Y. Lei, X. Gao, C. Ma, et al., Calcium carbonate supersaturation and precipitation in Chinese mitten crab (*Eriocheir japonica sinensis*) larval ponds in China: mass mortality, crystal form analysis, and safety saturation index, Aquaculture 272 (2007) 361–369.
[30] W. Wang, W. Gu, G.E. Gasparich, K. Bi, et al., Spiroplasma eriocheiris sp. nov., associated with mortality in the Chinese mitten crab, *Eriocheir sinensis*, Int. J. Syst. Evol. Microbiol. 61 (4) (2010) 703–708.
[31] C. Qu, Q. Xu, M. Lu, F. Wang, et al., The involvement of suppressor of cytokine signaling 6 (SOCS6) in immune response of Chinese mitten crab *Eriocheir sinensis*, Fish Shellfish Immunol. 72 (2018) 502–509.
[32] L. Song, C. Bian, Y. Luo, L. Wang, et al., Draft genome of the Chinese mitten crab, *Eriocheir sinensis*, GigaScience 5 (1) (2016) 5.
[33] T.D. Schmittgen, K.J. Livak, Analyzing real-time PCR data by the comparative CT method, Nat. Protoc. 3 (6) (2008) 1101–1108.
[34] B. Yang, Y. Jia, Z. Jia, W. Wang, et al., The cyclin-dependent kinase 2 (CDK2) mediates hematopoiesis through G1-to-S transition in Chinese mitten crab *Eriocheir sinensis*, Dev. Comp. Immunol. 81 (2018) 156–166.
[35] P.K. Smith, R.I. Krohn, G.T. Hermanson, A.K. Malla, et al., Measurement of protein using bicinchoninic acid, Anal. Biochem. 150 (1) (1985) 76–85.
[36] S. Jiang, Z. Jia, H. Chen, L. Wang, et al., The modulation of haemolymph arginine kinase on the extracellular ATP induced bactericidal immune responses in the pacific oyster *Crassostrea gigas*, Fish Shellfish Immunol. 54 (2016) 282–293.
[37] V. Deretic, T. Saitoh, S. Akira, Autophagy in infection, inflammation and immunity, Nat. Rev. Immunol. 13 (10) (2013) 722–737.
[38] S. Kawano, R. Umemiya-Shirafuji, D. Boldbaatar, K. Matsuoka, et al., Cloning and characterization of the autophagy-related gene 6 from the hard tick, *Haemaphysalis longicornis*, Parasitol. Res. 109 (5) (2011) 1341–1349.
[39] K. Suzuki, T. Kirisako, Y. Kamada, N. Mizushima, et al., The pre-autophagosomal structure organized by concerted functions of APG genes is essential for autophagosome formation, EMBO J. 20 (2001) 5971–5981.
[40] W. Feng, S. Huang, H. Wu, M. Zhang, Molecular basis of Bcl-xL's target recognition versatility revealed by the structure of Bcl-xL in complex with the BH3 domain of Beclin-1, J. Mol. Biol. 372 (1) (2007) 223–235.
[41] M.D. Lavine, M.R. Strand, Insect hemocytes and their role in immunity, Insect Biochem. Mol. Biol. 32 (2002) 1295–1309.
[42] Z.Y. Zhao, Z.X. Yin, S.P. Weng, H.J. Guan, et al., Profiling of differentially expressed

genes in hepatopancreas of white spot syndrome virus-resistant shrimp (*Litopenaeus vannamei*) by suppression subtractive hybridisation, Fish Shellfish Immunol. 22 (5) (2007) 520–534.
[43] I. Arsov, X. Li, G. Matthews, J. Coradin, et al., BAC-mediated transgenic expression of fluorescent autophagic protein Beclin 1 reveals a role for Beclin 1 in lymphocyte development, Cell Death Differ. 15 (9) (2008) 1385–1395.
[44] Y. Xu, C. Jagannath, X.D. Liu, A. Sharafkhaneh, et al., Toll-like receptor 4 is a sensor for autophagy associated with innate immunity, Immunity 27 (1) (2007) 135–144.
[45] J. Wang, X. Feng, Y. Zeng, J. Fan, et al., Lipopolysaccharide (LPS)-induced autophagy is involved in the restriction of *Escherichia coli* in peritoneal mesothelial cells, BMC Microbiol. 13 (1) (2013) 255.
[46] S. Valanne, J.H. Wang, M. Ramet, The *Drosophila* Toll signaling pathway, J. Immunol. 186 (2) (2011) 649–656.
[47] M. Hedengren, B.A. Sling, M.S. Dushay, I. Ando, et al., Relish, a central factor in the control of humoral but not cellular immunity in *Drosophila*, Mol. Cell 4 (1999) 827–837.
[48] W.C. Comb, P. Cogswell, R. Sitcheran, A.S. Baldwin, IKK-dependent, NF-κB-independent control of autophagic gene expression, Oncogene 30 (14) (2011) 1727–1732.
[49] P.H. Wang, Z.H. Gu, D.H. Wan, B.D. Liu, et al., The shrimp IKK-NF-kB signaling pathway regulates antimicrobial peptide expression and may be subverted by white spot syndrome virus to facilitate viral gene expression, Cell. Mol. Immunol. 10 (2013) 423–436.
[50] H.G. Boman, Antibacterial peptides: basic facts and emerging concepts, J. Intern. Med. 254 (2003) 197–215.
[51] J.F. Lan, J. Zhou, X.W. Zhang, Z.H. Wang, et al., Characterization of an immune deficiency homolog (IMD) in shrimp (*Fenneropenaeus chinensis*) and crayfish (*Procambarus clarkii*), Dev. Comp. Immunol. 41 (4) (2013) 608–617.
[52] Y. Zhang, L. Wanga, L. Wang, J. Yang, et al., The second anti-lipopolysaccharide factor (*Es*ALF-2) with antimicrobial activity from *Eriocheir sinensis*, Dev. Comp. Immunol. 34 (2010) 945–952.
[53] E. de-la-Re-Vega, A. Garcia-Galaz, M.E. Diaz-Cinco, R.R. Sotelo-Mundo, White shrimp (*Litopenaeus vannamei*) recombinant lysozyme has antibacterial activity against Gram negative bacteria: *Vibrio alginolyticus, Vibrio parahemolyticus* and *Vibrio cholerae*, Fish Shellfish Immunol. 20 (3) (2006) 405–408.